Exploring scale-effects on water balance components and water use efficiency of toposequence rice fields in Northern Italy

[Short title: **Water use efficiency of toposequence rice fields in Northern Italy**]

Facchi A.[(1)], Rienzner M.[(1)], Cesari de Maria S.[(1)], Mayer A.[(1)], Chiaradia E.A.[(1)], Masseroni D.[(1)], Silvestri S.[(2)], Romani M.[(2)]

[(1)] *Department of Agricultural and Environmental Sciences (DiSAA), Università degli Studi di Milano, Via Celoria 2, 20133, Milano (MI), Italy*

[(2)] *Centro Ricerche sul Riso, Ente Nazionale Risi (ENR), Strada per Ceretto 4, 27030, Castello d'Agogna (PV), Italy*

Corresponding author: Facchi A., arianna.facchi@unimi.it

KEYWORDS: rice, water balance terms, water use efficiency, toposequence, percolation, seepage, Darcy's equation

ABSTRACT

Water use efficiencies (WUEs) between 20% and 60% are commonly reported for single rice paddies. When larger spatial domains are considered, higher WUE than minimum values observed for individual fields are expected due to water reuse. This study investigates scale effects on water balances and WUEs of four adjacent rice fields located in Northern Italy and characterized by different elevations (A≅B>C>D). Water balance terms for the paddies were quantified during the agricultural season 2015 through the integrated use of observational data and modelling procedures. Following a Darcy-based approach, percolation was distinguished from net seepage. Results showed a net irrigation of about 2,700 and 2,050 mm for fields A and B, and around 640 and nearly 0 mm for C and D. WUE of A, B, C and D amounted, respectively, to 21, 28, 66 and >100%. Values for C and D were due to less permeable soils, to seepage fluxes providing extra water inputs and to the shallow groundwater level. When the group of paddies ACD were considered (B was not included since separated by a deep channel), net irrigation and WUE were found to reach 1,550 mm and 39%, confirming the important role of water reuses in paddy agro-ecosystems.

INTRODUCTION

Rice is one of the most important food crops worldwide, the last FAO statistic shows that rice ranked second in food and agricultural commodities, with a global production of more than 700 million tons per year (FAOSTAT, 2013). Italy is the largest rice producer in Europe, with the main production concentrated in the Po river plain (Northern Italy), in a vast area between Lombardy and Piedmont regions (about 250,000 hectares).

As widely known, rice cropping systems generally require copious amounts of water when the traditional irrigation management is adopted, due to the continuous flooding of rice paddies from seeding to a couple of weeks before harvest in order to maintain a ponded water level of 5-10 cm over the soil (Bouman et al., 2007; Cesari de Maria, 2017). Owing to this peculiar water management, rice usually requires from two to three times more water than other cereals, such as wheat or maize (Tuong et al., 2005). However, water use of flooded rice (i.e. the sum of irrigation and rainfall) may vary significantly due to the site characteristics, ranging from a relatively low value of 650-850 mm for some Asian paddies (e.g. Cabangon et al., 2004; Tabbal et al., 2002) up to a water use of more than 2500 mm observed in European experiments (e.g. Cesari de Maria et al., 2017; Aguilar and Borjas, 2005). Nevertheless, almost all the literature regarding water use and water balance of rice fields relates to studies performed in Asia, where puddling (i.e. harrowing or rotavating under shallow submerged conditions) is performed to reduce soil permeability, and only very few references focus on European rice cropping systems (Cesari de Maria et al., 2017; Zhao et al., 2015; Playán et al. 2008, Aguilar and Borjas, 2005), which are very different with respect to climate, soil types, rice varieties, irrigation management and agronomic practices. Consequently, there is the need to fill this research gap and to provide numbers to European water resource managers and to the public opinion, accusing rice cultivation of being excessively water-consuming.

Numerous are the factors influencing the water balance terms in a paddy, such as irrigation management, land preparation method, layout of the field, soil characteristics, agronomic management, crop characteristics, groundwater depth, rainfall amount and timing, and the evaporative power of the

atmosphere deriving from climatic conditions. Many water balance terms can be directly measured in the field (i.e., rainfall, irrigation inflow, irrigation outflow, water storage within and above the soil, evapotranspiration) as shown, for instance, in Cesari de Maria et al. (2017). The residual term of the water balance equation (*SP*) can be considered as the sum of two processes: net percolation, which is the net vertical flux at the bottom of the soil volume (mainly directed downward, since the continuous water flux toward the groundwater table basically prevents capillary rise into the root zone in flooded rice fields), and net seepage, defined as the subsurface flow of water (losses plus incoming fluxes) throughout the bunds (Bouman et al., 2007). In flooded rice fields, seepage is influenced by many factors, such as the position and slope of soil layers, their hydraulic conductivity, the presence of drains and their characteristics, the characteristics of bunds surrounding the field (thickness, presence of cracks, lining) and the water table depth and velocity (FAO, 1979). On the other hand, percolation is mostly influenced by the resistance to water movement in the soil profile, which is mainly governed by the saturated conductivity of the plough pan, (Bouman et al., 2007) and by the difference in water head along the vertical profile.

Compared to the other terms of the water balance, *SP* is the one most affecting rice water requirements. In general, the literature reports that total *SP* in a paddy may vary between 25-50% of the water inputs (i.e. irrigation plus rainfall) with heavy soil and groundwater depth within 0.5 m (Cabangon et al., 2004; Dong et al., 2004), and 80% in coarse-textured soil with a groundwater table deeper than 1.5 m (Sharma et al., 2002; Singh et al., 2002).

Since *SP* can not be measured directly in field-scale experiments and is usually obtained as the residual term of the water balance, it is a challenge for research to separate *SP* into the two fluxes. According to Wopereis (1994), the soil vertical profile some days after flooding can be described as a sequence of layers. Following a downward order, the layers are: i) ponding water, ii) muddy layer with low resistance to water flow, iii) plough sole layer with a relevant resistance to water flow, iv) subsoil layer scarcely affected by agronomical practices. After flooding, the muddy layer and the plough sole are saturated; in this condition, the percolation rate *P* can be predicted by the Darcy's equation (Rizzo et al., 2013). This approach is commonly adopted in the literature and it is implemented, among the others, in the Darcy-based soil-water balance model SAWAH

(Simulation Algorithm for Water Flow in Aquatic Habitats; Ten Berge et al., 1992) to calculate the amount of water that percolates from paddy fields.

A widely adopted indicator to measure the efficiency of an irrigated system is the water use efficiency (WUE), which is obtained as the ratio of evapotranspiration to water inputs (i.e. irrigation plus rainfall). Tuong and Bhuiyan (1999) report that WUE of flooded rice can be as low as 20%, even though with remarkable variations (upper bound of the range is 60%). Since *SP* generally increases the field irrigation requirements of a rice paddy, WUE of a single field is strongly influenced by the water amount lost by *SP*. When focusing on larger spatial domains, WUE is expected to increase compared to the minimum values found for single paddies, due to the possible water reuse within the system. Hafeez et al. (2007) and Wallace (2000) report increased values of water use indicators considering, respectively, the district and the catchment scales. At a larger scale than the single field, *SP* outflowing from fields can be partially collected by ditches, thus increasing the irrigation discharge available for downhill paddies. Additionally, *SP* can also represent a direct water input to fields at a lower elevation, due to seepage through the bunds. In rain-fed rice, Tsubo et al. (2006) observed that water losses by lateral movements were greater in the upper part of the rice field toposequence, and that these lateral fluxes represented a possible water gain for fields at a lower elevation, affecting also their field WUE. Similarly, Schmitter et al. (2015) found that the field position in the toposequence influenced the crop water productivity in case of irrigated rice, due to subsurface lateral fluxes that represented and extra water input for the lower lying fields. Moreover, lower paddies may benefit form a higher groundwater level that plays an important role in reducing percolation fluxes when groundwater is shallow (Cesari de Maria et al., 2016; 2017; FAO, 1979).

Hence, in paddy areas, topography is a factor activating water exchanges and reuse between paddies. For this reason, WUE of a single rice field in a toposequence tends to be poorly representative of the overall efficiency of the paddy system, especially in areas characterized by shallow groundwater, due to the strong interactions that may occur among fields. In spite of its relevance, this issue is still not much investigated in the literature and, to the authors' knowledge, no experiments leading to a quantification of water fluxes and WUE for paddies in a toposequence have been conducted in European rice areas.

106 The aim of this paper is to provide procedures and elements for the investigation of scale-effects when
107 considering the water balance terms and the water use efficiency of flooded rice systems in a toposequence.
108 To reach the objective, the water balance terms of four rice paddies characterized by different elevations
109 and located in the most important paddy area in Italy (Lomellina rice district, Northern Italy) were quantified
110 through the integrated use of observational data and modelling procedures. Net irrigation discharges,
111 percolation and seepage fluxes of the four fields are discussed with respect to their position in the
112 toposequence, together with WUEs considering both the single-field scale and the group of rice paddies.
113

114 **MATERIAL AND METHODS**

115 **Description of the site**

116 The study was carried out in the Cerino rice farm (Semiana, Pavia) located in Lomellina, a historical rice
117 district situated in the western Lombardy plain, southwest of the city of Milan. The area is characterized by
118 a humid subtropical climate (Cfa) according to the Köppen climate classification. Considering the period 1993-
119 2015, the mean temperature in the months from April to September is around 19.6°C, while the total rainfall
120 is about 310 mm. The average daily reference evapotranspiration (ET_0) of the same period, as calculated from
121 Allen et al. (1998), is 3.6, 4.5, 5.2, 5.8, 4.2, 3.1 mm d^{-1}, respectively.
122 The monitoring activity was performed in 2015 in three adjacent paddy fields, named A, C and D, and in an
123 additional field, named B, separated from the others by a deep drainage channel. The area of the four fields
124 (A, B, C, D) is, respectively, 7.8, 8.2, 4.8, and 5.8 ha. The elevation of the fields decreases from A (94.0 m
125 a.s.l.), to C (about 1 m below A), and D (about 0.5 m below C); B has an elevation of 93.8 m a.s.l.. Figure 1
126 shows a plan view and cross sections of the study area. In the rice district of Northern Italy, bunds are
127 permanent (not ploughed) and decades of clogging due to the flooding practice generally made them rather
128 impervious. In the experimental farm, bunds surrounding the block of fields ACD (apart from the southern
129 one), and field B (apart from the northern one) are about five meters large at the seedbed level, and often
130 flanked by farm roads, as can be seen in Figure 1. The remaining bunds are thinner, with a thickness of about
131 two meters at the seedbed level.

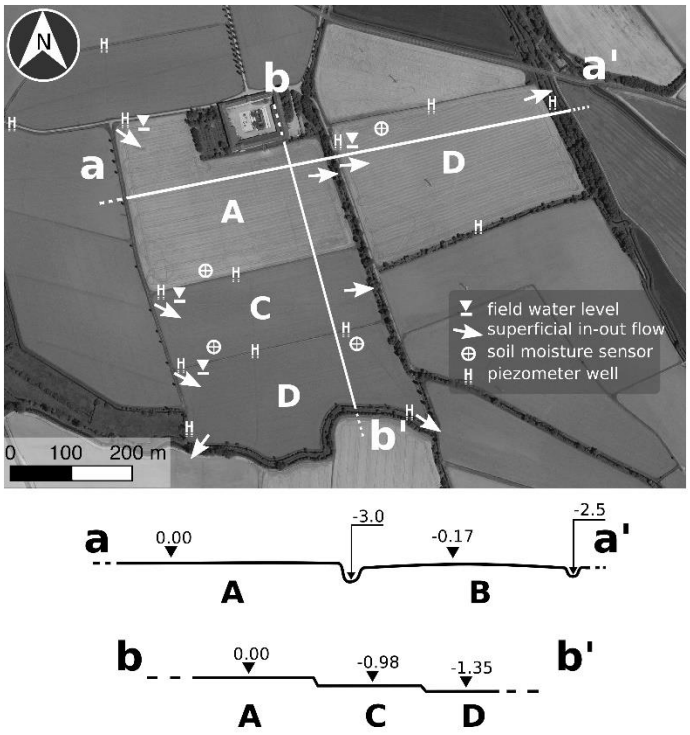

Figure 1 - Plan view and cross sections of the monitored fields with the position of the installed instruments

Before sowing, the four paddies were harrowed and subsequently rolled. Fields A and B were planted with the rice variety Sole CL, while fields C and D with the variety CL 15. Both the varieties are characterized by a growing cycle of 135-140 days.

A different irrigation management was adopted for the four paddies: water seeding and continuous flooding (WFL) was applied in C and D, while dry seeding and delayed flooding (i.e. direct seeding on dry soil followed by a delayed flooding when the crop reaches the 3-4 leaf stage; DFL) was adopted for A and B. After submersion, the ponding water was maintained in all the fields for approximately the entire growing cycle, except for short periods when agronomic operations were conducted. In particular, a first dry period was necessary in fields C and D to allow the root development and, successively, dry periods were performed for all the fields to allow the application of fertilizers and pesticide treatments. Figure 2 illustrates flooding periods (dots) and seeding and harvesting dates (x) of the four paddies. Despite the different irrigation management of fields A and B compared to C and D, the overall length of the flooding period was approximately the same for the four fields.

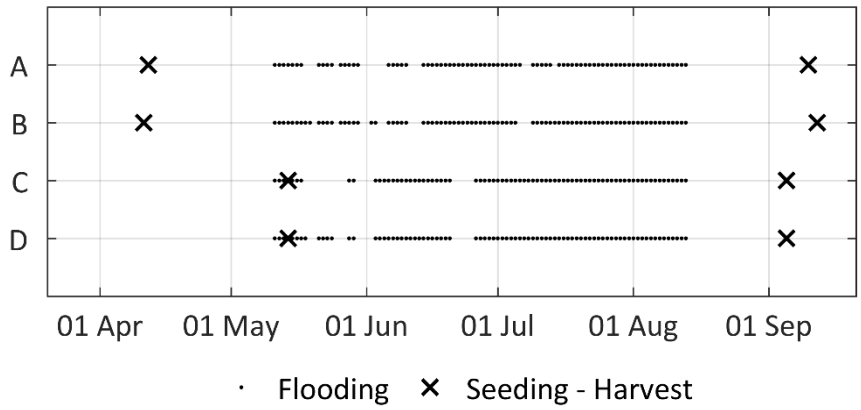

Figure 2 - Flooding periods and seeding and harvesting dates for paddies A, B, C and D in the agricultural season 2015 at the Cerino rice farm (Semiana, Pavia)

Experimental setup and data collection

For investigating the water dynamics within the four fields, a sensors network was set up in each field (Figure 1) to monitor the following water fluxes and storages: irrigation inflow, irrigation outflow, ponding water height, soil water content, and water table depth. All the measurements were continuously recorded by different data loggers during the whole crop cycle, with a time step of 10 to 30 minutes.

Irrigation inflows and outflows at each field were measured by long-throated flumes equipped with a level gauge (Chiaradia et al., 2015). The flumes were self-made, and dimensioned to fit the expected maximum discharge of 80 l s^{-1} (rectangular-shaped, 1.2 m long, 0.3 m wide and 0.4 m high). Flow rate curve was estimated by using the WinFlume software (U.S.B.R., USA). Upstream water levels were measured in stilling wells by pressure transducers having a full scale of 0.30 Bar (Keller, Switzerland). A total of nine long-throated flumes were installed: four to measure irrigation inflows at the four fields, and five for monitoring the irrigation outflows (field D has two irrigation outlets).

The ponding water height was measured by pressure transducers (full scale of 0.30 Bar; Keller, Switzerland) installed in the four fields. The soil water content was monitored in each field at four soil depths (10, 30, 50, 70 cm) by multi-level FDR (Frequency Domain Reflectometry) probes (EnviroSCAN, Sentek, Australia).

168 Water table depth was monitored through a total of fourteen piezometers made by windowed 1''1/5 PVC
169 pipes installed into holes drilled using a manual auger. Twelve piezometers were equipped with a pressure
170 transducer (Keller, Switzerland ; STS, USA; Van Essen Instrument, The Netherlands), while the two remaining
171 were monitored weekly through manual measurements. For each monitoring time step, the measured
172 groundwater levels were interpolated on a regular grid with 10 m x 10 m cells (Natural Neighbor Interpolation
173 method; MATLAB, The Mathworks, USA).
174 Between March and May 2015, a geophysical survey with an EMI device (GSSI Profiler-EMP400) and a
175 traditional soil survey (40 drillings carried out with a manual auger) were conducted to obtain a preliminary
176 description of soil physical characteristics and distribution. For each drilling, disturbed soil samples were
177 taken at three depths (0-30, 40-80 and 90-130 cm) for textural analysis. Soil of the four fields shows a
178 significant uniformity in the tilled horizon (top 30 cm), with a sandy loam texture, whereas a higher textural
179 variability (from sandy to silty clay loam) is evident below this horizon. All the information collected in the
180 preliminary soil survey was used to identify areas potentially characterized by different soil types and to
181 select the more representative sites for an in-depth soil characterization. In November 2015, five two-meter-
182 deep soil profiles were opened with an excavator and characterized (two profiles in field A, two in field B,
183 and one in field C). Disturbed soil samples were taken from each soil horizon for chemical-physical soil routine
184 analysis, and undisturbed soil samples were collected at the same positions for the determination of bulk
185 density. Large undisturbed soil cores (height 15.0 cm, ø 14.6 cm, two replicates) were taken from the less
186 conductive layer (LCL) of each profile (often being the hardpan) for the laboratory determination of the
187 saturated soil hydraulic conductivity. Depth and thickness of LCL were observed for each profile by
188 considering different features (e.g. soil compaction, transition between layers showing reductive features –
189 above- and oxidative conditions –below).
190 The soil survey highlighted a narrow area crossing the central part of field B, characterised by a relatively
191 coarser soil with respect to the other two portions of the field. Unfortunately, a soil profile was not opened
192 in this area, but information about LCL position and texture could be obtained by drillings.

193 In field D, drainage is strongly impeded and water is ponding on the soil surface for nearly the whole year;
194 therefore, it was impossible to open a profile in November 2015. However, the preliminary soil survey and
195 the installation of piezometric wells allowed to detect a thick and compact clayey layer about 1.2 meters
196 below the soil surface, that acts as the less conductive layer and is most likely responsible for the poor
197 drainage of field D.
198 Finally, hourly meteorological data (air temperature and humidity, rainfall, wind speed, solar radiation) were
199 obtained by the closest regional weather station, 12 km far from the experimental site.
200
201 **Calculation of balance terms**
202 For each field, a balance equation (Eq. 1) was implemented at an hourly time step from dry seeding till harvest
203 in case of DFL treatments (A and B), and from the first flooding before wet seeding till harvest for WFL ones
204 (C and D). A field control volume ranging from the top of the ponding water to the bottom of the LCL was
205 considered (this means that control volumes are different for the four fields, see Table 1).
206
207 $$\Delta S_{w,t} + \Delta S_{s,t} = Q_{in,t} - Q_{out,t} + R_t - ET_t + SP_t \quad (1)$$
208
209 where: t is the time index (h), ΔS_w is the variation in the ponding water height; ΔS_s is the variation of the soil
210 water storage; Q_{in} and Q_{out} are the irrigation inflow and outflow divided by the field area; R is the rainfall; ET
211 is the evapotranspiration from soil/ponding water (evaporation) and crop (transpiration); SP is the seepage
212 and percolation term discussed in the introduction. All the terms are in mm h^{-1}. Positive signs indicate an
213 increasing storage or a flux entering the soil volume in the time step.
214 Seepage and percolation (SP) can be split as follows:
215
216 $$SP_t = Se_t - P_{bal,t} \quad (2)$$
217

where *Se* (mm h^{-1}) is the seepage flux, positive when the inflow is higher than the outflow, and P_{bal} (mm h^{-1}) is the vertical flux at the bottom of the LCL, that can be both negative (downward) and positive (upward). However, in flooded fields, a continuous downward flow of water from the soil surface to below the LCL (called 'percolation') basically prevents capillary rise, and a positive vertical flux is found only in case of high-pressure groundwater below the LCL. On the contrary, when paddies are dry, the flow at the bottom of the LCL can become positive (capillary rise) if the water table is sufficiently shallow.

Most of the terms in Eq. 1 were measured, while the remaining terms were calculated as described hereafter. *ET* was estimated following the FAO single crop coefficient approach (Eq. 3) (Allen et al., 1998), considering a complete fulfilment of the crop evapotranspiration requirements:

$$ET_t = K_{c,t} \cdot ET_{0,t} \quad (3)$$

The reference evapotranspiration (ET_0) was computed from hourly meteorological data following Allen et al. (2006), while time-varying crop coefficients (K_c) were obtained for the two irrigation managements, WFL (Kc_{ini} = 0.8, Kc_{mid}= 1.1, Kc_{end}= 0.6) and DFL (Kc_{ini} = 0.6, Kc_{mid}= 1.1, Kc_{end}= 0.6) from a former experiment carried out on rice under the same irrigation treatments in a study site nearby (12 km) (Cesari de Maria et al., 2017; Chiaradia et al., 2015).

The *SP* term was not monitored and it was obtained by applying Eq. 1. Furthermore, if one of the two components, *Se* or P_{bal}, can be estimated independently, then Eq. 2 can be applied to estimate the other one. An estimation of the percolation P_{bal} was obtained, in this study, by applying the 1D Darcy's equation (Eq. 4) during the field submersion (ponding water on the soil surface > 0), when most of the percolation is expected to occur:

$$P_{D,t} = b \cdot K_s \cdot \frac{\Delta H_t}{L} \quad (4)$$

where: P_D is the percolation (mm h^{-1}) calculated from the Darcy's law, *Ks* is the saturated hydraulic conductivity of LCL (cm d^{-1}), *L* is the thickness of LCL (cm), *b* is a conversion factor (10/24 mm d cm^{-1} h^{-1}), and Δ*H* (cm) is the difference in the total hydraulic head at the two LCL sides:

$$\Delta H_t = H_{2,t} - H_{1,t} \quad (5)$$

where H_1 (cm) and H_2 (cm) are the total hydraulic heads at the top and the bottom of the LCL, respectively. For fields characterized by different soil zones (i.e. A and B), the total percolation was obtained by weighing the percolation fluxes obtained for the different soil zones by their surface areas.

The LCL properties (*Ks* and *L*) were investigated for the soil profiles representative of the different soil zones; in particular, *Ks* was determined on large undisturbed soil cores by applying the core method in laboratory (e.g. Reynolds and Elrick, 2002). The hydraulic heads H_1 and H_2 were estimated for each soil zone along the flooding period as described hereafter.

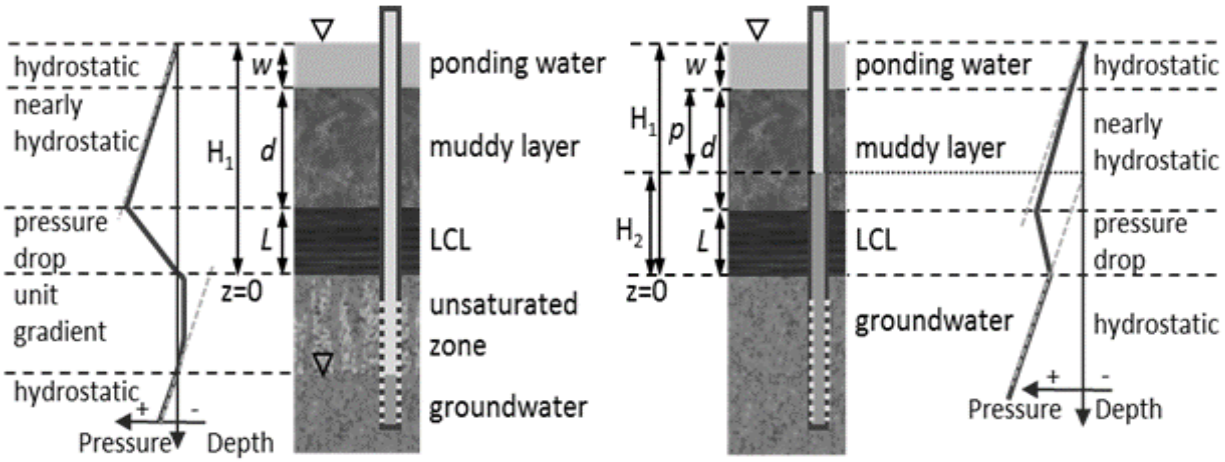

Figure 3 - Scheme of the application of the 1D Darcy's equation in case the layer below LCL is, respectively, unsaturated (left-hand side) or saturated (right-hand side); qualitative pressure head profiles are also illustrated

Since the muddy layer above the LCL is typically incoherent and highly conductive (Wopereis et al., 1994), its effect on the flux can be neglected in computing Eq. 4. When the LCL is deeper than 30 cm, a soil layer may be placed between the incoherent muddy layer and the LCL, but also its effect on the percolation can be neglected since its *Ks* is usually higher than the LCL by far.

With respect to Figure 3, when the reference level *z*=0 is placed at the bottom of the LCL, the total hydraulic head at the top of the *LCL* (H_1) can be approximated as:

$$H_{1,t} = w_t + d + L \quad (6)$$

where: *w* (cm) is the height of the ponding water, *d* (cm) is the depth of the LCL from the soil surface, and *L* (cm) is its thickness; all the quantities on the right-hand side of Eq. 6 were measured in the field.

The total hydraulic head at the bottom of the LCL (H_2) was computed according to the water table position with respect to LCL, as shown in Figure 3.

In case of unsaturated soil below the LCL (Figure 3, left-hand side), a negative water pressure occurs below the LCL, whereas the LCL is supposed to be fully saturated (i.e. water pressure ≥ 0). Therefore, being H_2 the water pressure at the interface between these layers, its value can be assumed equal to zero.

In case of a complete saturation of the soil profile (Figure 3, right-hand side), the soil below the LCL is saturated, its pressure head is positive and increases with depth following a hydrostatic pressure gradient and H_2 is equal to the distance between the groundwater level and the bottom of the LCL (Eq. 7):

$$H_{2,t} = d + L - p \quad (7)$$

where $p = \left(z_s - z_{w,t}\right)$ (cm) is the distance between the soil surface and the groundwater table computed for each time step. In this case, P_D can become positive if $H_2 > H_1$.

Obviously, ΔH values change for the four fields at each monitoring step, as the ponding water height and the groundwater depth fluctuates.

Since a measure of *Ks* was unavailable for the LCL of the soil unit in the central part of the field B, an estimation was carried out by calibrating this parameter in order to obtain, at the end of the agricultural season, a P_D value equal to the *SP* cumulative flux, assuming that no net seepage occurred for field B as a consequence of its topographic position (in analogy to what was observed for field A).

Finally, *Ks* and thickness of LCL in field D were set to reproduce the negligible observed percolation flux; *Ks*, in particular, was set to a very low value.

Table 1 reports the main soil physical and hydrological properties of the LCLs used in the computation of percolation (P_D) through the Darcy's approach. For each row of parameters, Table 1 also reports the fraction of the area of the field they apply to (according to the soil survey described in the previous Section).

Table 1 – Main soil physical and hydrological properties of LCLs of the fields (d - depth, L - thickness, Ks - saturated hydraulic conductivity, Texture following USDA classification, BD - bulk density)

Field	Field fraction	*d* (cm)	*L* (cm)	*Ks* (cm d^{-1})	Texture	*BD* (g cm^{-3})
A	0.23	30	5	0.342	Sandy Loam	2.05
	0.77	55	25	1.020	Loam	2.00
B	0.30	20	5	0.017	Sandy Loam	1.98
	0.37	20	15	1.700*	Sandy Loam	-
	0.43	40	15	0.145	Loam	1.93
C	1.00	45	7	0.057	Loam	1.98
D	1.00	120	40	0.001*	Clay Loam	-

* estimated

The approach for computing P_D was applied only in periods when paddy fields were submerged (ponding water on the soil surface > 0). In this case, *Se* was estimated from the cumulative *SP* - P_D curve by manual calibrating a stepwise linear interpolant, the slope of which is equal to the *Se* value in each time step. *Se* values estimated for each step were also evaluated in the light of the observational data collected in the field.

306 P_{bal} was consequently set as $SP - Se$. During non-flooding periods (ponding water on the soil surface = 0), the
307 net seepage was assumed to be negligible (Se = 0), and the net flux at the bottom of LCL was obtained as the
308 residual term in the water balance equation (P_{bal} = SP; Eq. 1); in this case, positive P_{bal} indicates a capillary
309 rise flux into the soil unit volume. In non-flooding periods, P_D = P_{bal} was furthermore imposed in order to
310 maintain a complete P_D series.
311 When the group of paddies ACD is considered, terms of the water balance are calculated from those of the
312 three fields, weighted by their surfaces.
313 All the equations reported in this Section were implemented in a MATLAB script.
314
315 **Computation of Water Use Efficiencies**
316 The water use efficiency (WUE, %) was calculated for each paddy, as well as for the group of paddies ACD,
317 with the modified index proposed by Dunn and Gaydon (2011):
318
319 $$WUE = 100 * \frac{ET}{Q_{in} - Q_{out} + R} \quad (8)$$
320
321 where ET, Q_{in} and Q_{out} are expressed in mm over the whole agricultural season. The irrigation outflow (Q_{out})
322 was subtracted from the total water inputs (Q_{in} +R) because the irrigation outflow is discharged into the
323 irrigation network and is consequently reused for the irrigation of paddy fields located downslope. It shall be
324 noted that the WUE of a group of fields does not correspond to the average of the WUEs of single fields. In
325 particular, the WUE of a group of paddies is reported on the left-hand side of Eq. 9, while the area-weighted
326 average of the single WUEs is illustrated on the right-hand side of Eq. 9:
327
328 $$\frac{\sum A_i \cdot ET_i}{\sum [A_i (R + Q_{in,i} - Q_{out,i})]} * 100 \neq \sum \left(\frac{A_i}{A} \cdot \frac{ET_i}{R + Q_{in,i} - Q_{out,i}} \right) * 100 \quad (9)$$
329
330 where A_i is the area of the single fields (m^2), while A is the area of the group of fields (m^2). All the remaining
331 terms (ET, R, Q_{in}, Q_{out}) are also expressed in meters.

RESULTS AND DISCUSSION

Monthly water balance terms

Water balance terms are presented in Figure 4 at a monthly time scale, water volumes entering the fields have positive values, while outgoing volumes have negative values. Some terms are only slightly visible (e.g. ΔS_s and ΔS_w), but all are reported for sake of completeness. During the flooding period, average groundwater depths at the experimental site were found to be around 0.8, 1.2, 0.1 and 0.6 m in fields A, B, C, and D, respectively.

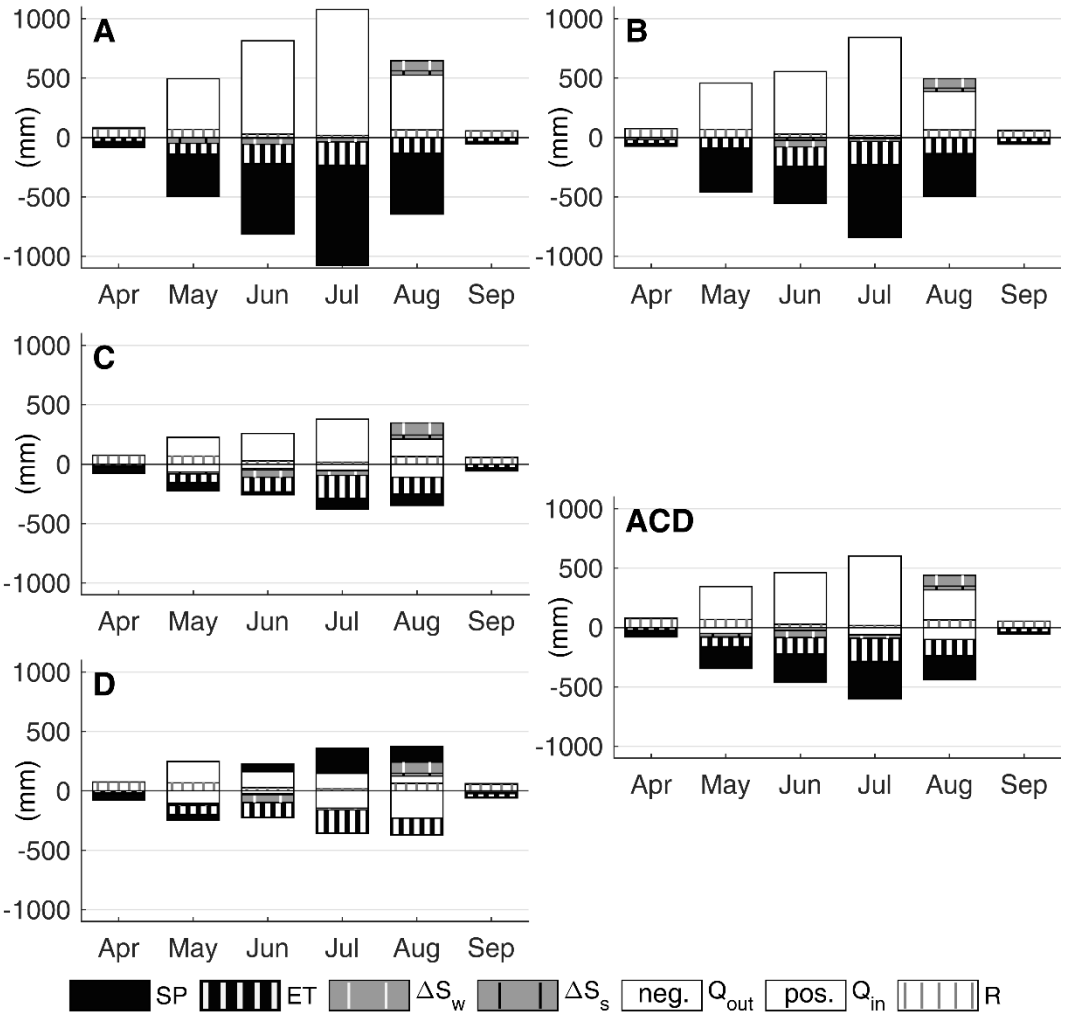

Figure 4 - Monthly cumulated water balance terms for fields A, B, C, D and the group of fields ACD: SP - seepage and percolation, ET – evapotranspiration, ΔS_w - change in water storage on the field, ΔS_s - change

344 *in water storage within the soil, Q_{out} – irrigation outflow (negative), Q_{in} – irrigation inflow (positive), R -*

345 *rainfall*

346

347 In Figure 4, fields A and B (DFL) show a very similar pattern characterized by large water fluxes mostly due,
348 inward, to the irrigation supply (Q_{in}) and, outward, to the seepage and percolation term (*SP*).
349 Evapotranspiration (*ET*) is smaller than Q_{in} and the irrigation outflow (Q_{out}) is nearly absent. The amounts
350 reached by Q_{in} and *SP* during the season follow the number of flooding days, reaching a maximum in July
351 (Figure 2). The maximum of *ET*, occurring in July too, is due to the meteorological factors affecting ET_0. Finally,
352 the storage terms (ΔS_s and ΔS_w) have negative values at the start of the season (i.e. water is stored on and
353 within the soil) and positive at drying (i.e. the stored water is released). Field C (WFL) shows common
354 features to A and B, but with remarkably smaller Q_{in} and *SP* fluxes. Moreover, Q_{out} is often rather relevant in
355 this field, especially in August. The pattern of fluxes in field D (WFL) is different with respect to the other
356 monitored fields. Indeed, Q_{in} has the same magnitude of *ET* and it is often smaller than Q_{out}; the reason of
357 this is a relevant and positive *SP* flux. The maximum of Q_{in} occurs in May, which is the only month where *SP*
358 is negative in D, while the maximum positive *SP* is reached in July. Finally, when the group ACD is considered,
359 water fluxes and storages appear to have an average behaviour between those shown for A and C.

360

361 **Breakdown of the *SP* term into seepage and percolation fluxes**

362 The complex behaviour identified for the balance terms in the previous Section can be better explained by
363 dividing *SP*, calculated as the residual of the water balance (Eq. 1, Figure 4), into its vertical and horizontal
364 components, namely percolation (P_{bal}) and seepage (*Se*), respectively (Eq. 2).
365 Figure 5 illustrates *SP* fluxes cumulated over the agricultural season (bold black line), and P_D fluxes (bold grey
366 line), estimated by applying the Darcy's law. The figure also illustrates the cumulative patterns of *Se* (dotted
367 black line) and P_{bal} (thin black line) fluxes obtained by partitioning *SP*. On the x-axis, periods of flooded
368 conditions, as obtained by water level sensors positioned in each field, are additionally reported (the
369 correspondence between these periods and those reported in Figure 1, having the aim to illustrate the water

management operated by the farmer, is not always perfect as periods in Figure 1 do not account for short time submersions due to heavy rainfall events on nearly saturated soil).

In case of field A, a very good correspondence was found between *SP* and P_D fluxes, with respect to both the cumulative value of the two variables at the end of the season and the seasonal trend. Actually, no incoming seepage was expected in this field due to its high topographic position, and Figure 5a suggests that also outward seepage can be considered negligible. Consequently, *Se* was assumed to be null throughout the season, and thus $P_{bal} = SP$.

For field B (Figure 5B), the matching between P_D and *SP* cumulative values at the end of the season is due to the calibration of the *Ks* value of the coarser soil crossing the central portion of the field. Anyway, the overall seasonal patterns of the two fluxes have a very good match, with SP that does not show sharp short-term deviations from P_D estimation. This allowed to discard the hypothesis of relevant seepage fluxes affecting B; these fluxes were set to zero in analogy with field A, also due to a similar position of the two fields with respect to the adjacent fields and to the groundwater level.

The cumulated patterns of *SP* and P_D for field C (Figure 5C) are divergent, due to the presence of relevant seepage fluxes. By comparing the cumulative ($SP - P_D$) curve for the fields C and D (not shown), a good correspondence between the sudden slope changes in the two lines was evident in different time periods. In particular, changes were found to have the same behaviour but different sign (i.e. a decrease in the curve of field C corresponded to an increase in the cumulative ($SP - P_D$) curve for field D), and this suggested a water flux from C to D in these periods. The first occurrence corresponded to a large break of the embankment between the two fields (about 30 l s^{-1} on average from 1-July-2015 to 2-July-2015) also observed in the field, while the second was a proper seepage flux (about 3 l s^{-1} from 30-July-2015 to 15-Aug-2015). Both can be noted by observing the *Se* line in Figure 5C and 5D.

Field D was characterized by an irrelevant P_D flux compared to the other three fields (Figure 5D); thus, *SP* was mostly due to *Se* during the flooding periods. In addition to the two seepage fluxes coming from C, the cumulated *SP* flux showed an additional rise from 16-June-2015 (one day after the main submersion in A) to 19-Aug-2015 (4 days after the drying of fields A and C) with an average flux of 3.0 l s^{-1}. This period was

396 characterised by a groundwater level measured by piezometers on the bund between C and D higher than
397 the ponding water in D (not shown). Therefore, a groundwater flux entering D above its LCL was added to
398 the *Se* term. Finally, a flux outgoing from D to the adjacent drainage channel occurred from 11-Aug-2015 to
399 17-Aug-2015 (6.0 l s^{-1}), reducing the slope of the *SP* curve just before the field drying (mid-August). After the
400 removal of the identified *Se* fluxes from *SP*, the cumulated values of P_{bal} and P_D matched fairly well also for
401 fields C and D (Figure 5C e 5D).
402

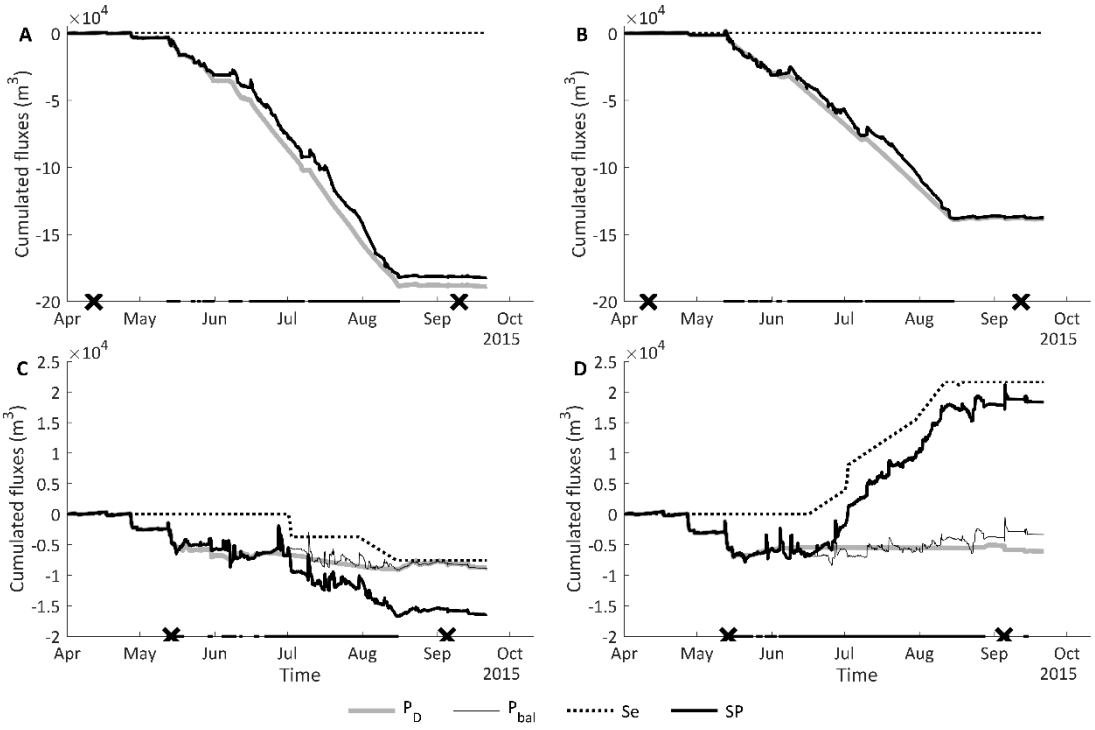

403

404 *Figure 5 – Daily cumulated fluxes of SP, P_D, Se and P_{bal} for fields A, B, C and D; panels have different Y scales.*
405 *On the X axis, black dots show periods with water ponding in the fields, while seeding and harvesting dates*
406 *are marked with X*
407

408 **Seasonal water balance and WUE at different scales**

409 Table 2 reports the cumulated fluxes on a seasonal basis. Values are referred to the period from seeding to
410 harvest for fields A and B (152 and 155 days respectively), and from the very first submersion of the season
411 (just before seeding) to harvest for fields C and D (117 days). Since the periods are different, also the total
412 amount of precipitation (*R*) and evapotranspiration (*ET*) differs slightly among the fields. The ΔS_s and ΔS_w

terms are very small and they are reported in Table 2 for sake of completeness. Contrarily, relevant amounts and strong differences among the fields appear when comparing Q_{in}, Q_{out} and WUE.

In fields A and B, water infiltrates at a high rate; thus, fields can be dried for treatment application just by stopping the irrigation inflow for one or two days. Due to these high infiltration rates, Q_{out} was always close to zero. On the contrary, the farmer used the irrigation outlets of C and D during the season to control the water level in the field and to dry the fields as required by treatments. In case of field D, Q_{out} was practically equal to Q_{in}, due to the presence of lateral fluxes. High irrigation inputs and negligible discharges led to high net irrigations (Q_{in} - Q_{out}) required by A (2710 mm) and B (2050 mm), whereas net irrigation input was only 640 mm in C and almost no irrigation was required in D.

Considering only the irrigation management adopted in the fields, DFL applied to A and B resulted in lower WUEs (21 and 28%, respectively) compared to the traditional WFL technique adopted in C and D (66 and 275%, respectively). Although some studies comparing WFL and DFL report small water savings in case of DFL (e.g. Cesari de Maria et al., 2017; Borrell et al., 1997), DFL showed a much lower WUE than WFL in this study, due to the topographic position of fields A and B and to the high permeability of their soils. Since farmers often select fields where applying DFL management on the basis of the permeability of their soils and the groundwater table depth (tillage operations must be conducted in these fields by means of common agricultural machinery), DFL applied in the real agricultural world may often not achieve WUEs observed in experimental tests.

Leaving aside the peculiar condition of field D, WUEs observed for fields A, B and C are in good agreement with results of other studies. With respect to experiments performed in Northern Italy, WUE according to data from Zhao et al. (2015) ranged from a minimum of 26% and a maximum of 56%, similarly to values computed from Karpouzas et al. (2005), varying between 28% and 60% in two subsequent years. On the other hand, values closer to the lower bound are reported by Cesari de Maria et al. (2017) and Aguilar and Borjas (2005) who observed WUEs between 17% and 27% for flooded rice paddies. As found for many other countries, a lower WUE of paddies compared to other cereals can be observed also in Northern Italy. In particular, the WUE of maize, which is the major crop cultivated in the Po river plain, usually ranges between

30 and 50% when border irrigation is applied and to 70 to 80 % in case of sprinkler irrigation (data from regional reports).

Table 2- Seasonal water balance terms (mm) and WUE (%) for fields A, B, C, D and for the group of paddies ACD, computed from seeding to harvest for field A e B and from the first submersion (a few days before seeding) to harvest for fields C and D

Field	*R*	Q_{in}	Q_{out}	Net irr.	ΔS_s	ΔS_w	*ET*	*SP*	WUE
A	273	2716	6	2710	10	0	630	-2327	21
B	273	2067	17	2050	13	0	635	-1660	28
C	198	899	261	638	6	0	575	-277	66
D	198	504	501	3	19	0	575	387	275
ACD	273	1544	230	1315	6	0	611	-972	39

Since the very high WUE of field D is due to extra water inputs provided by the continuous flooding of fields A and C, water balance terms and WUE were computed also considering the group of paddies A, C and D as a whole (ACD in Table 2). Due to the internal reuse of seepage fluxes occurring between paddies, the net irrigation of the group of fields ACD (around 1550 mm) was indeed lower than that measured for A and B, while WUE was found to be around 40%.

CONCLUSIONS

This study focused on the quantification of water balance terms and water use efficiency (WUE) of four rice fields, characterized by different elevations (A ≅ B > C > D) and located in the main Italian rice basin (Lomellina region), during the agricultural season 2015. Irrigation water management was dry-seeding and delayed flooding (DFL) in fields A and B, and water seeding and continuous flooding (WFL) in fields C and D. Since fields A, C and D lay on the same slope (while B is separated by a deep drainage channel) and their water dynamics are often interconnected, the three fields were also considered as a whole (ACD) in the study.

During the entire agricultural season, a higher net irrigation was required by the upslope fields A (2,710 mm) and B (2,050 mm) compared to downslope fields C (638 mm) and D (nearly 0 mm). The small values for the fields C and D are not only due to a low soil permeability and a shallow groundwater table, but also to the occurrence of incoming seepage fluxes from upslope fields.

By measuring or estimating the different terms of the water balance for each field, the seepage and percolation flux (*SP*) was computed as the residual term of the water balance equation. Following a Darcy-based approach, percolation could be distinguished from net seepage. Throughout the flooding periods, *SP* was found to be practically coincident with the percolation term for the upslope fields (A and B), and no significant seepage fluxes were identified for these fields. On the contrary, seepage provided a large amount of water to the downslope field D, which was characterized by an irrelevant vertical percolation due to both a low soil permeability and a very shallow groundwater table, most likely maintained by the percolation of the upslope fields (A and C). Field C behaved halfway between fields A and D. The net irrigation for the group of paddies ACD reached 1,550 mm, due to the water reuse within paddies in the toposequence.

WUEs of the upslope fields (A and B) were 21-28%, field D showed a WUE > 100%, while an intermediate value was found for field C (66%). Considering the irrigation management adopted in the fields, DFL applied to A and B resulted in lower WUEs compared to the traditional WFL technique adopted in C and D. This was due to the fact that, in the specific case study, topography was the dominant factor in determining the value of WUE, overwhelming all the other factors, including the irrigation management. The group ACD showed a relatively high WUE (39%), due to water reuse among fields promoted by the topographic gradient. This demonstrates that none of the fields could be considered representative for the entire paddy area, and thus, to quantify the WUE of a sequence of fields on a slope, the monitoring scale must be enlarged to include all the fields in the area.

ACKNOWLEDGEMENTS

483 This study was conducted in the context of the project WATPAD, funded by Fondazione Cariplo (grant n°
484 2014-1260) which is kindly acknowledged. We wish to thank Paolo Carnevale, owner of the Cerino farm (PV),
485 for hosting the experimentation.

486

487 **REFERENCES**

488 Aguilar M., Borjas F., 2005. Water use in three rice flooding management systems under Mediterranean
489 climatic conditions. Span. J. Agric. Res. 3 (3): 344–351.

490 Allen R.G., Pereira L.S., Raes D., Smith M. 1998. Crop evapotranspiration—guidelines for computing crop
491 water requirements. In: FAO Irrigation andDrainage Paper 56. Food and Agriculture Organization, Rome

492 Allen R.G., Pruitt W.O., Wright J.L., Howell T.A., Ventura F., Snyder R., Itenfisu D., Steduto P., Berengena
493 J., Yrisarry J.B., Smith M., Pereira L.S., Raes D., Perrier A., Alves I., Walter I., Elliott R. 2006. A recommendation
494 on standardized surface resistance for hourly calculation of reference ETO by the FAO56 Penman-Monteith
495 method. Agr. Water Manage. 81:1-22. DOI : 10.1016/j.agwat.2005.03.007

496 Borrell A., Garside A., Fukai S., 1997. Improving efficiency of water use for irrigated rice in a semi-arid
497 tropical environment. Field Crop Res. 52:231–248

498 Bouman B.A.M., Lampayan R.M., Tuong T.P. 2007. Water management in irrigated rice; coping with water
499 scarcity. International Rice Research Institute, Los Baños. ISBN 978-971-22-0219-3

500 Cabangon R.J., Tuong T.P., Castillo E.G., Bao L.X., Lu G., Wang G.H., Cui L., Bouman B.A.M., Li Y., Chen C.,
501 Wang J. 2004. Effect of irrigation method and N-fertilizer management on rice yield, water productivity and
502 nutrient-use efficiencies in typical lowland rice conditions in China. Paddy Water Environ. 2:195–206

503 Cesari de Maria S., Bischetti G.B., Chiaradia E.A., Facchi A., Miniotti E.F., Rienzner M., Romani M., Tenni
504 D., Gandolfi C. 2017. The role of water management and environmental factors on field irrigation
505 requirements and water productivity of rice. Irrig. Sci. 35:11-26. DOI: 10.1007/s00271-016-0519-3

506 Cesari de Maria S., Rienzner M., Facchi A., Chiaradia E.A., Romani M., Gandolfi C. 2016 Water balance
507 implications of switching from continuous submergence to flush irrigation in a rice-growing district.
508 Agricultural Water Management, 171:108–119. DOI: 10.1016/j.agwat.2016.03.018

509 Chiaradia E.A., Facchi A., Masseroni D., Ferrari D., Bischetti G.B., Gharsallah O., Cesari de Maria S., Rienzner
510 M., Naldi E., Romani M., Gandolfi C. 2015. An integrated, multisensor system for the continuous monitoring
511 of water dynamics in rice fields under different irrigation regimes. Environ. Monit. Assess. 187(9):586. DOI:
512 10.1007/s10661-015-4796-8

513 Dong B., Molden D., Loeve R., Li Y.H., Chen C.D., Wang J.Z. 2004. Farm level practices and water
514 productivity in Zanghe Irrigation System. Paddy Water Environ. 2:217–226

515 Dunn B.W., Gaydon D.S. 2011. Rice growth, yield and water productivity responses to irrigation scheduling
516 prior to the delayed application of continuous flooding in south-east Australia. Agr. Water Manage. 98:1799–
517 1807

518 FAO, 1979. Land evaluation criteria for irrigation. Report of an Expert Consultation, 27 February-2 March,
519 1979. World Soil Resources Report No. 50. FAO Rome. 219 p.

520 FAOSTAT 2013. Food and agriculture organization of the United Nations, statistics division. Download
521 data: http://faostat3.fao.org/download/Q/QC/E. Accessed Jan 2015

522 Hafeez M.M., Bouman B.A.M., Van de Giesen N., Vlek P., 2007. Scale effects on water use and water
523 productivity in a rice-based irrigation system (UPRIIS) in the Philippines. Agr. Water Manage. 92:81-89

524 Karpouzas D., Ferrero A., Vidotto F., Capri E., 2005. Application of the RICEWQ-VADOFT model for
525 simulating the environmental fate of pretilachlor in rice paddies. Environ. Toxicology and Chem. 24 (4):1007-
526 1017

527 Playán E., Pérez-Coveta O., Martínez-Cob A., Herrero J., García-Navarro P., Latorre B., Brufau P., Garcés J.,
528 2008. Overland water and salt flows in a set of rice paddies. Agr. Water Manag. 95:645–658

529 Reynolds WD, Elrick DE. 2002. 3.4.2.2 Constant Head Soil Core (Tank) Method, pag 804 in “Mehods of Soil
530 Analysis part 4 – Physical methods. SSSA book series: 5”. Soil Science Society of America, Inc. Madison,
531 Wisconsin, USA

532 Rizzo A., Boano F., Revelli R., Ridolfi L. 2013. Role of water flow in modeling methane emissions from
533 flooded paddy soils. Adv. Water Resour. 52:261–274

534 Schmitter P., Zwart S.J., Danvi A., Gbaguidi F., 2015. Contributions of lateral flow and groundwater to the
535 spatio-temporal variation of irrigated rice yields and water productivity in a West-African inland valley. Agr.
536 Water Manage. 152:286-298

537 Sharma P.K., Lav Bhushan, Ladha J.K., Naresh R.K., Gupta R.K., Balasubramanian B.V., Bouman B.A.M.
538 2002. Crop-water relations in rice-wheat cropping under different tillage systems and water management
539 practices in a marginally sodic, medium-textured soil. In: Bouman B.A.M., Hengsdijk H., Hardy B., Bindraban
540 P.S., Tuong T.P., Ladha J.K. (eds) Water-wise rice production. International Rice Research Institute, Los Baños,
541 pp 223–235

542 Singh A.K., Choudhury B.U., Bouman B.A.M. 2002. Effects of rice establishment methods on crop
543 performance, water use, and mineral nitrogen. In: Bouman B.A.M., Hengsdijk H., Hardy B., Bindraban P.S.,
544 Tuong T.P., Ladha J.K. (eds) Water-wise rice production. International Rice Research Institute, Los Baños, pp
545 237–246

546 Tabbal D.F., Bouman B.A.M., Bhuiyan S.I., Sibayan E.B., Sattar M.A. 2002. On-farm strategies for reducing
547 water input in irrigated rice; case studies in the Philippines. Agric. Water Manage. 56: 93–112

548 Ten Berge H.F.M., Jansen,D.M., Rappoldt K., Stol. W. 1992. The soil water balance module SAWAH: user's
549 guide and outline. CABO-TPE Simulation Reports, Vol. 22

550 Tsubo M., Basnayake J., Fukai S., Sihathep V., Siyavong P., Sipaseuth, Chanphengsay M. 2006.
551 Toposequential effects on water balance and productivity in rainfed lowland rice ecosystem in Southern Laos.
552 Field Crop. Res., 97: 209–220

553 Tuong T.P., Bhuyyan S.I. 1999. Increasing Water-use efficiency in rice production: Farm levels
554 perspectives. Agric. Water Manage. 40:117:122

555 Tuong P., Bouman B.A.M., Mortimer M. 2005. More Rice, Less Water—Integrated Approaches for
556 Increasing Water Productivity in Irrigated Rice-Based Systems in Asia. Plant Prod. Sci. 8:231-241, DOI:
557 10.1626/pps.8.231

558 Wallace J.S. 2000. Increasing agricultural water use efficiency to meet future food production. Agr.
559 Ecosyst. Environ. 82:105–119

560 Wickham T.H., Singh V.P. 1978. Water movement through wet soil. In: Soil and Rice. International Rice
561 Research Institute, Los Banos, Philippines, pp. 337±357

562 Wopereis M.C.S., Bouman B.A.M., Kropff M.J., ten Berge H.F.M. Maligaya A.R. 1994. Water use efficiency
563 of flooded rice fields I. Validation of the soil-water balance model SAWAH. Agr. Water Manage. 26: 277-289

564 Zhao Y., De Maio M., Vidotto F., Sacco D., 2015. Influence of wet-dry cycles on the temporal infiltration
565 dynamic in temperate rice paddies. Soil Till. Res. 154: 14–21